PAPER

Atropisomerism of a monosubstituted perfluoro[2.2]paracyclophane. A combined synthetic, kinetic, spectroscopic and computational study†

Ion Ghiviriga, Henry Martinez, Christian Kuhn, Lianhao Zhang and William R. Dolbier, Jr.*
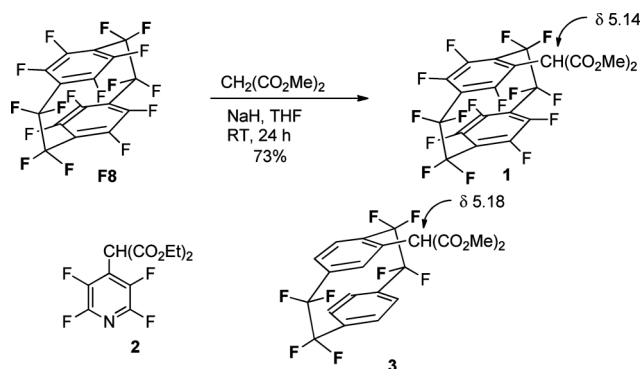
The product of S_NAr addition of the enolate of ethyl acetoacetate to perfluoro[2.2]*para*-cyclophane exists entirely as its enol tautomer **5**. This enol exhibits two NMR signals for its enolic proton, and these signals were shown to derive from the presence of two, equal energy conformations that were observable as distinct, stable conformations at room temperature, but which when heated, interconverted with an energy barrier of 23.5 kcal mol^{-1}. These atropisomers were characterized by NMR, with details of this analysis being provided. Computational work corroborated the NMR conclusions, and provided additional insight into all structural, thermodynamic and kinetic results. Enol product **5** was cyclized, under basic conditions, to form a benzofuran product **6**. Its structure was confirmed by NMR, with further structural and mechanistic insights being provided by calculations.

Introduction

It has been demonstrated that perfluoro[2.2]paracyclophane (**F8**) exhibits high reactivity in reactions with nucleophiles such as hydroxide, methoxide, benzenethiolate, and dimethyl malonate anion.[1] On the basis of direct competitive studies, using methoxide as nucleophile, its reactivity was found to be much greater than that of hexafluorobenzene, but considerably less than that of pentafluoropyridine.

In its reaction with four equivalents of dimethyl malonate anion, a single product, 4-bis(carbomethoxy)methyl-perfluoro[2.2]paracyclophane (**1**) was obtained in 73% yield after stirring at RT for two days (Scheme 1).[1] Likewise the reaction of diethyl malonate anion with pentafluoropyridine has been reported to produce 4-bis(carboethoxy)methyl-2,3,4,5-tetrafluoropyridine (**2**) in 33% yield after heating in DMF at 100 °C for 4 hours.[2] The mechanisms for these reactions were both assumed to be the normal S_NAr mechanism. The analogous adduct (**3**) of 1,1,2,2,9,9,10,10-octafluoro[2.2]-paracyclophane (**AF4**) had been prepared *via* an assumed $S_{RN}1$ reaction of the dimethyl malonate anion with 4-iodo-AF4.[3] Each of these products appears to exist exclusively as the bis-ester tautomer, with no NMR evidence of the presence of its enol tautomer. Proton spectra of the two [2.2]paracyclophane adducts (**1** and **3**), exhibited one proton singlets at 5.14 and 5.18 ppm, respectively, for the carbinyl C–H protons, with no evidence of any signal in the region of 13–14 ppm where the enolic protons would be expected to appear.

Department of Chemistry, University of Florida, P.O. Box 117200, Gainesville, FL 32611-7200, USA. E-mail: wrd@chem.ufl.edu
† Electronic supplementary information (ESI) available. See DOI: 10.1039/c1ob06157g

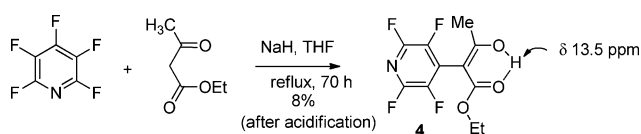**Scheme 1** Malonic ester derivatives.

All monosubstituted [2.2]paracyclophanes, such as **1** and **3**, are, of course, chiral and because of this the two carbomethoxy groups of compounds **1** and **3** are diastereotopic, with the methyl protons appearing in the case of **1** as individual singlets at 3.78 and 3.88 ppm, and in the case of **3** at 3.61 and 3.98 ppm.

In contrast to these malonic ester derivatives, the analogous acetoacetic ester derivative of pentafluoropyridine (**4**) appears to exist entirely in its enol tautomeric form, as evidenced by its proton NMR spectrum.[4] Ethyl 3-hydroxy-2-(perfluoropyridin-4-yl)but-2-enoate (**4**), is a single, presumably *Z*-isomer, exhibiting a singlet in the proton NMR at 13.52 ppm for its enolic hydrogen, with no evidence of a signal for a carbinyl C–H. It was obtained, albeit in low yield, from the reaction of ethyl acetoacetate enolate anion with pentafluoropyridine (Scheme 2).[4]

At this time we wish to report a similar acetoacetic ester derivative of **F8**, which not only exists exclusively in its enol form, but also is a slowly equilibrating mixture of atropisomers.

Scheme 2 Reaction of pentafluoropyridine with ethyl acetoacetate enolate anion.

Results and discussion

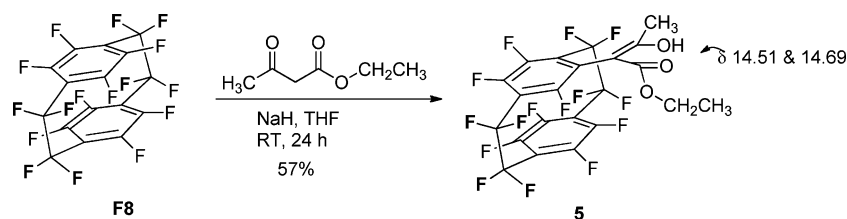### Reaction of enolate anion with F8 and initial consideration of enolic product 5

When **F8** was allowed to react with the enolate anion of ethyl acetoacetate for about 24 h at room temperature in THF, a 57% yield of pure enol product (**5**) was obtained (Scheme 3), as evidenced by the lack of any signal in the vicinity of 5.14 ppm. Instead, two signals were observed in the enolic region, at 14.51 and 14.69 ppm along with two signals for the ketonic methyl group at 1.43 and 2.08 ppm, the latter being, surprisingly, a broad triplet. The nature of the two species responsible for these signals was not immediately apparent.

The existence of acetoacetic ester derivatives **4** and **5** in exclusively enolic form is worthy of some discussion. Ethyl acetoacetate is known to exist as a mixture of keto-enol tautomers, the exact ratio of which appears to be significantly dependent upon concentration and choice of solvent. About 8% of enol is accepted as the value obtained by NMR in chloroform (Scheme 4).[5]
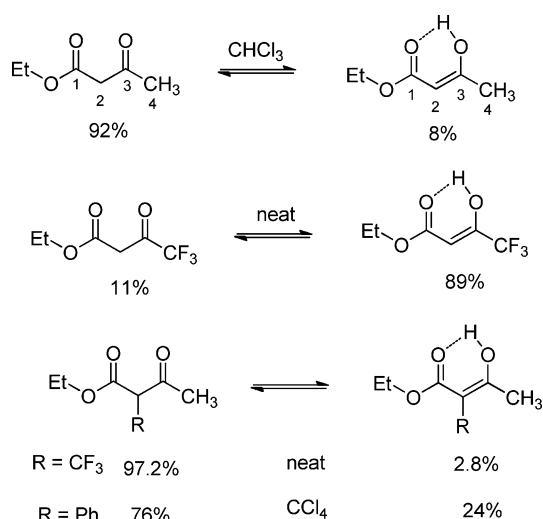
When an inductively withdrawing group such as CF_3 replaces the CH_3 group at the 4-position, destabilization of the carbonyl group gives rise to a large increase in the relative amount of enol present at equilibrium (89%),[6] whereas when a CF_3 substituent is attached at the 2-position, the amount of enol at equilibrium decreases significantly (2.8%).[7] On the other hand, placing a phenyl substituent at the 2-position appears to somewhat stabilize the enol, relative to the keto tautomer, with 24% of the enol being observed in CCl_4.[8]

What is now apparent based on the above observations for both Sandford's perfluoropyridyl derivative (**4**) and our **F8** derivative (**5**) is that replacing a 2-phenyl substituent with a *strongly electron-deficient* heteroaryl or aryl substituent provides sufficient extra stabilization of the enolic tautomer to make it the exclusively observed tautomer.

The issue then remains to explain why pyridyl derivative **4** exhibits only one enolic signal in the proton NMR, whereas **F8**-derivative **5** exhibits two. A combination of NMR, computational and kinetic evidence will be seen to demonstrate that the two enolic forms of **5** derive from (a) the *chirality* of monosubstituted [2.2]paracyclophanes combined with (b) a sufficiently *sterically-crowded* environment at the position of substitution in **5** to inhibit

Scheme 4 Keto-enol tautomerism of some substituted ethyl acetoacetates.

C–C single bond rotation of the enol substituent. If the barrier to such single bond rotation is large enough, then it will be possible for the compound to exist in two diastereoisomeric forms, or atropisomers, as distinguishable diastereomers interconverted by single bond rotation are called.

It is thus proposed that **F8**-derivative **5** exists as a pair of atropisomers (diastereomers **5a** and **5b**), which are sterically inhibited from interconverting, mainly by interactions with the bridge CF_2 group most proximate to it (at C-2), Fig. 1.
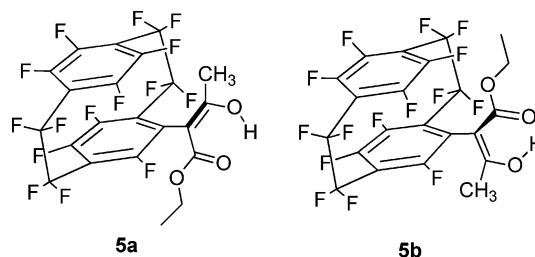

Fig. 1 Depiction of atropisomers of F8-acetoacetic ester enol derivative **5**.

Kinetics of 5a–5b thermal interconversion

The two atropisomers were isolated as an approximately 1.5 to 1 mixture of crystalline products. When placed in solution, the **5a** and **5b** underwent slow thermal equilibration. In order to measure the rate constant for this interconversion, the relative concentrations of **5a** → **5b** were monitored in benzene-d_6 at 25 °C

Scheme 3 Reaction of **F8** with enolate of ethyl acetoacetate.

by ^{1}H-NMR for 18 h. The slope of the plot ln([5a]–[5a]$_{eq}$), which is the natural logarithm of the difference between the concentration of **5a** at time t and its concentration at equilibrium, *vs.* time is equal to the sum of the rate constants for the forward and backward reactions, $k_f + k_b$. Since the equilibrium constant, $K = k_f/k_b$ was observed to be 1.0, $k_f = k_b = 3.67 \times 10^{-5}$ ($\pm 0.07 \times 10^{-5}$) s^{-1}, which corresponds to a half-life of 5.25 h at 25 °C.

Since none of the signals gave any indication of coalescence in benzene-d$_6$ at 75 °C, the barrier for rotation was measured by nOe difference experiments, in tetrachloroethylene-d$_2$, using the method of Forsen and Hoffman.[9,10] Limited solubility precluded the use of ^{13}C signals at natural abundance; therefore proton signals were used, and as a consequence the data suffer from the interference of the nOe's. MB(∞), the remaining fraction of the intensity of the signal of H4′ in **5a** when H4′ in **5b** is irradiated long enough to reach equilibrium, was monitored in a nOe difference experiment at 95, 115, and 125 °C. Using these data, the barrier to rotation ($\Delta G^{\ddagger}_{298}$) was calculated to be 23.5 (± 1.1) kcal mol^{-1}. Using this value for $\Delta G^{\ddagger}$, the calculated value for k at 25 °C is 3.65 $\times 10^{-5}$ s^{-1}, which is remarkably close to the actual measured value, which was discussed in the previous paragraph.

Cyclization of F8-enolate

When the mixture of **5a** and **b** was treated with NaH and heated overnight at 50 °C in THF, a cyclized product, **6**, was formed in 52% yield, presumably *via* an intramolecular S$_N$Ar reaction of the enolate (Scheme 5).
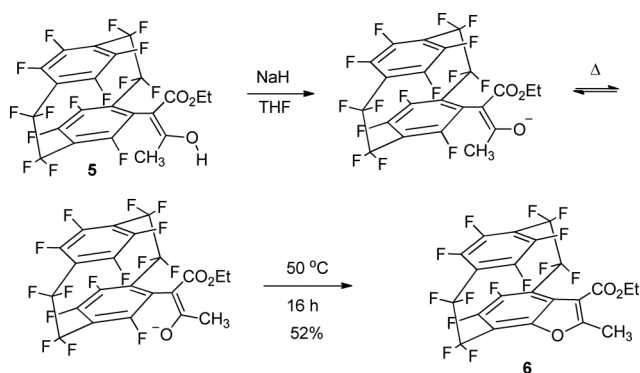
Scheme 5 Cyclization of the enolate of **5**.

Although Sandford pointedly did not observe a similar cyclization of the perfluoropyridyl analog **4**, related cyclizations were observed with tetrafluoropyrazine and pyridazine to give cyclized products **7** and **8** in 71% and 40% yields, respectively (Fig. 2).[4] Likewise, in much earlier work, ketone enolates were observed to cyclize in two stage reactions with hexafluorobenzene to give products such as **9** (29% yield).[11,12]
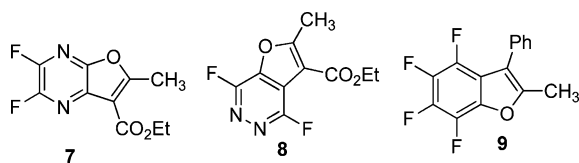

Fig. 2 Cyclization products from reaction of acetoacetic ester enolate with tetrafluoropyrazine and tetrafluoro pyridazine and of 1-phenyl-propanone with hexafluorobenzene.
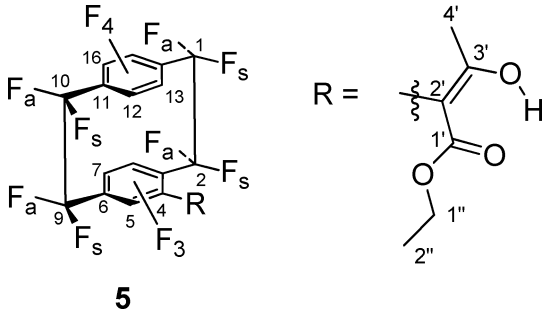
NMR characterizations

The ^{1}H spectrum of compound **5** in benzene-d_6 at 25 °C displays the presence of two species, **5a** and **5b**, in an initial ratio of 1.50, which after 18 h reaches an equilibrium with a ratio of 1.00. Both of these species are monosubstituted perfluoro[2.2]paracyclophanes (PFPCs), as indicated by the observation of eight bridge and seven aromatic fluorine signals for each in their ^{19}F NMR spectra (all pertinent NMR spectra are provided in the Supplementary Information†). The chemical shifts of their respective OH protons (14.51 ppm in **5a** and 14.69 ppm in **5b**) and of their C2′ carbons (94.2 and 94.4 ppm) indicate that the *beta*-ketocarboxylate moiety is in the enol form for both compounds, with an intramolecular, resonance assisted hydrogen bond.

The ^{1}H and ^{13}C chemical shifts for both *beta*-ketocarboxylate moieties have been assigned based on the ^{1}H-^{13}C gHMBC spectrum, which displayed cross-peaks between both the OH and H4′ protons and C3′ and C2′, and also between H1″ and C1′.

The assignments of the ^{19}F chemical shifts in Table 1 were based on the ^{19}F–^{19}F couplings, measured in selectively decoupled TOCSY1D spectra and confirmed by the ^{19}F–^{19}F DQCOSY spectrum, using methodology that has been described earlier.[13] In the first step, cross-peaks in the DQCOSY spectrum identified the bridge fluorine geminal pairs, *a1–a7*, *a2–a5*, *a3–a6* and *a4–a8*. These represent the signals in **5a**, numbered in decreasing order of their chemical shifts (*a-1* to *a-15*). Large couplings around 70 Hz ($^4J_{syn}$) identified the aromatic fluorines *ortho* and *syn* to some bridge fluorines, *a15* to *a5*, *a14* to *a6*, and *a9* to *a7*. Other smaller couplings ($^5J_{syn}$ around 10–30 Hz) of *a5*, *a6* and *a7* identified the aromatic fluorines *pseudo-geminal* to their *ortho* and *syn* partners, correspondingly *a12*, *a10* and *a13*, which in turn displayed a coupling around 20 Hz with the bridge protons *ortho* and *syn* to them, correspondingly *a4*, *a1* and *a3*. At this point there were four possibilities for joining the two half-PFPCs identified up to this stage. The aromatic fluorine *pseudo-geminal* to the substituent, *a11* displays cross-peaks in the DQCOSY spectrum with *a13* and *a14*, narrowing the possibilities to two, of which we retain the one in which the diagonal relationship of the coupling constants in the half-molecules is the same. Coupling constants relevant to the assignments that were made are presented in Tables 2, 3 and 4.

Both **5a** and **5b** have *three* $^4J_{syn}$ couplings that are larger than 50 Hz, which indicates that they exist in conformations where the upper deck is skewed away from the substituent.[13] This is to be expected because of the bulky substituent in **5**.

The ^{1}H–^{19}F HOESY spectrum demonstrates that **5a** and **5b** are atropisomers that exist because of restricted rotation about the C4–C2′ bond. In **5a**, H4′ appears in the proton spectrum as a broad triplet of *ca.* 4 Hz. The HOESY spectrum indicates that these couplings are with F5 and F13; therefore in **5a** the ketonic methyl group points towards the upper deck. Other cross-peaks in the HOESY spectrum demonstrate a coupling smaller than the line-width of H4′ with F2S and nOes between H4′ and F12 and between H2″ and F2A. In **5b**, the ethyl group points towards the upper deck, and the HOESY spectrum displays nOes between both (diastereotopic) H1″ protons and F12, between one of them and F13, and between H4′ and F9S, F2A and F8. Other COSY-type peaks of H2″ with F12, F13 and F5 and of H4′ with F5 confirm the relative geometry of **5b**.

Table 1 ^{1}H, ^{19}F and ^{13}C chemical shift (ppm) assignments for conformers **5a** and **5b** and for compound **6** in benzene-d_6 at 25 °C

5

Position	Compound **5a**				Compound **5b**			Compound **6**		
	δ ^{13}C	δ ^{19}F (signal label)	δ ^{1}H		δ ^{13}C	δ ^{19}F	δ ^{1}H	δ ^{13}C	δ ^{19}F (signal label)	δ ^{1}H
1S	nm^a	−97.90 (*a-2*)	—		nm	−98.28	—	nm	−99.73 (*a-1*)	—
1A	nm	−105.00 (*a-5*)	—		nm	−104.82	—	nm	−106.10 (*a-8*)	—
2S	nm	−107.99 (*a-8*)	—		nm	−106.89	—	nm	−101.26 (*a-3*)	—
2A	nm	−100.57 (*a-4*)	—		nm	−100.63	—	nm	−103.57 (*a-6*)	—
9S	nm	−106.53 (*a-7*)	—		nm	−106.84	—	nm	−103.54 (*a-5*)	—
9A	nm	−97.86 (*a-1*)	—		nm	−98.00	—	nm	−101.51 (*a-4*)	—
10S	nm	−99.23 (*a-3*)	—		nm	−99.50	—	nm	−100.99 (*a-2*)	—
10A	nm	−105.29 (*a-6*)	—		nm	−105.16	—	nm	−105.10 (*a-7*)	—
5	nm	−113.03 (*a-9*)	—		nm	−109.19	—	nm	—	—
7	nm	−123.68 (*a-10*)	—		nm	−124.46	—	nm	−133.05 (*a-11*)	—
8	nm	−131.26 (*a-12*)	—		nm	−130.77	—	nm	−130.49 (*a-10*)	—
12	nm	−131.79 (*a-13*)	—		nm	−132.35	—	nm	−136.00 (*a-14*)	—
13	nm	−129.83 (*a-11*)	—		nm	−127.41	—	nm	−130.10 (*a-9*)	—
15	nm	−134.42 (*a-15*)	—		nm	−135.03	—	nm	−135.02 (*a-13*)	—
16	nm	−134.28 (*a-14*)	—		nm	−134.89	—	nm	−135.00 (*a-12*)	—
1′	171.5	—	—		170.5	—	—	162.4	—	—
2′	94.2	—	—		94.4	—	—	112.4	—	—
3′	179.2	—	14.51^b		179.6	—	14.69^b	164.6	—	—
4′	21.0	—	2.08^c		19.8	—	1.43	12.7	—	2.12
1″	62.1	—	3.90^d 3.69^d		61.6	—	4.24^d 3.97^d	61.5	—	4.14
			4.05^d							
2″	13.3	—	0.83^e		13.8	—	1.05^e	13.8	—	1.02

^{a} not measured. ^{b} OH. ^{c} broad triplet, J = 4 Hz. ^{d} doublet of quartets, J = 11.0, 7.1 Hz. ^{e} triplet, 7.1 Hz.

Table 2 Selected ^{19}F–^{19}F coupling constants for atropisomer **5a** in benzene-d_6 at 25 °C

Position	^2J (Hz)	^3J (Hz)	$^4J_{syn}$ (Hz)	$^5J_{syn}$ (Hz)
1S	251	12 (F1S-F2S)	26	—
		13 (F1A-F2A)		
1A			74	28
2S	246		—	15
2A			18	0
9S	251	12 (F9S-F10S)	72	14
		10 (F9A-F10A)		
9A			17	0
10S	252		27	0
10A			69	19

Table 3 Selected ^{19}F–^{19}F coupling constants for atropisomer **5b** in benzene-d_6 at 25 °C

Position	^2J (Hz)	^3J (Hz)	$^4J_{syn}$ (Hz)	$^5J_{syn}$ (Hz)
1S	252		25	—
1A			70	31
2S	243		—	23
2A			17	0
9S	252	11 (F9S-F10S)	52	11
		10 (F9A-F10A)		
9A			21	0
10S	252		30	0
10A			67	13

The proton chemical shifts of the two atropisomers are consistent with a shielding region below the lower deck and a deshielding region between decks and out of the footprint of the aromatic ring, both of which are to be expected given the diamagnetic anisotropy of the benzene ring.

A conformational search in HyperChem, using AM1 for the energies, found two sets of conformations, the C3–C4–C2′–C1′ dihedral angle being 114–124° in one set, corresponding to **5b**, and −63° in the other. By AM1, **5b** is *ca.* 1 kcal mol^{-1} more stable than

5a (Note the more accurate calculation of these relative energies in the next section). The two conformations are depicted in Fig. 3.

The assignment of the ^{19}F signals of compound **6** was done in the same manner as for **5a** and **5b**. However, in this case the two half-PFPCs were joined based on the coupling between *a14* and *a9*, *ca.* 20 Hz. Two large $^4J_{syn}$ couplings indicate that **6** also prefers the 'away' conformation. Because of the *ortho*-disubstituted pattern in **6**, there are now two possibilities for assignment, *e.g.*, *a9* to F12 and *a14* to F13 or the other way around, *a9* to F13 and *a14* to F12. A heteronuclear nOe difference experiment in which H2″

This journal is © The Royal Society of Chemistry 2012

Org. Biomol. Chem., 2012, **10**, 882–889 | **885**

Table 4 Selected ¹⁹F–¹⁹F coupling constants for compound **6** in benzene-d_6 at 25 °C

Position	^2J (Hz)	^3J (Hz)	$^4J_{syn}$ (Hz)	$^5J_{syn}$ (Hz)
1S	253	7 (F1S-F2S)	20	—
1A			72	30
2S	252		—	32
2A			14	0
9S	252	8 (F9S-F10S) 9 (F9A-F10A)	—	8
9A			33	0
10S	253		36	0
10A			60	8
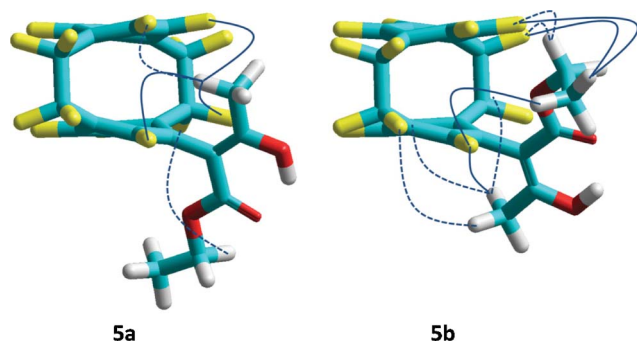
Fig. 3 Optimized geometries (AM1) for conformers **5a** and **5b**, with the interactions seen in the HOESY spectrum, scalar couplings (solid line) and nOes (dashed).

was selectively irradiated produced selective population transfer on the *a3* signal, which was assigned as F2S. Therefore the latter possibility (*a9* = F13 and *a14* = F12) appears to be the correct assignment of fluorines for compound **6**, with all other assignments following as given in Table 1.

Computational results

In order to provide supplementary support for the existence of approximately equal energy atropisomers for compound **5**, quantum chemical calculations were performed in the gas phase at both HF and B3LYP/6-31+G(d,p) levels of theory. The model compound used for these calculations replaced the ethyl with a methyl group in the ester function (see **5a′** and **5b′** in Fig. 4 and 5). In addition to calculating the ground state energy of the two atropisomers, the rotation energy barrier that led to their interconversion was calculated as well at the B3LYP/6-31+G(d,p) level.
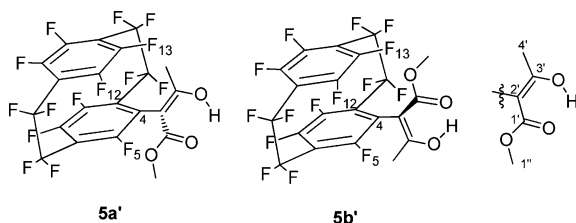
Fig. 4 Model structures used for calculations.

Also, in order to obtain additional mechanistic understanding of the cyclization reaction of **5** to produce **6**, a smaller, non-cyclophane model structure was used in order to minimize
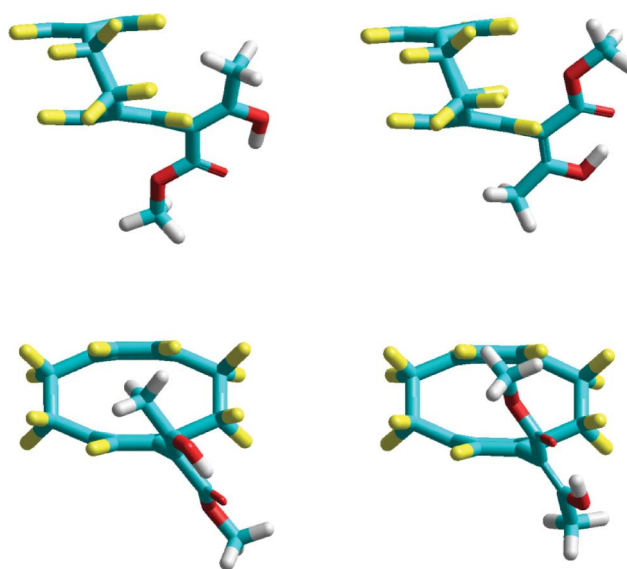
Fig. 5 Calculated ground states for **5a′** (left) and **5b′** (right) at B3LYP level.

computational time. The energy barriers of the transition states leading to cyclization product were calculated at B3LYP/6-31+G(d,p) level in the presence of THF as a solvent using the Polarizable Continuum Model (PCM). The transition states were characterized by only one imaginary frequency and the intrinsic reaction coordinate (IRC), connecting both the starting material and the product. All calculations were performed using the Gaussian 03 Rev. E01 package.[14]

The ground state calculations at both HF and B3LYP levels confirmed a small energy difference between the two atropisomers (Table 5). As expected the methyl 3-hydroxy-2-but-2-enoate substituent at the 4-position of **F8** is not planar with the ring, since there would be a strong repulsive interaction between the substituent and the closest CF_2 on the bridge. Even when not planar, the bulk of the substituent forces the upper deck ring away from the substituent in both atropisomer structures. According to the HF method, the more stable of the two atropisomers is **5b′**, while the B3LYP method shows a slight preference for **5a′**; in either case the energy difference is minimal (Table 5). Both atropisomers exhibit a strong hydrogen bond between the hydrogen of the enol and the carbonyl of the ester function.

The following discussion is based upon the results from the B3LYP method, but it would also similarly apply to the HF results.

The relevant computed geometrical data are presented in Table 6. The dihedral angles between C5–C1′ in both isomers suggest that the double bond of the enol has little to no conjugation with the aromatic ring. The distances between C4–C2′ in both isomers support this assumption since the length has more single than double bond character. For isomer **5a′**, the distances between the hydrogens of methyl C4′ and fluorines 12 and 13 in the upper

Table 5 Relative energies (kcal mol⁻¹) between **5a′** and **5b′** at both HF and B3LYP levels

	5a′	**5b′**
HF	0.3	0
B3LYP	0	0.16

Table 6 Relevant geometrical information of isomers **5a′** and **5b′**

	C4–C2′ (Å)	C1′–C5 (θ)	C2′–C3′ (Å)	H1″–F13 (Å)	H1″–F12 (Å)	H4′–F13 (Å)	H4′–F12 (Å)
5a′	1.49	121.06	1.39	—	—	2.50	2.38
5b′	1.49	−60.38	1.39	3.36	2.85	—	—

ring (2.38 and 2.50 Å, respectively) are within the sum of the Van der Waals radii of both hydrogen and fluorine, 1.20 Å and 1.47 Å, respectively. This in consistent with the observation that the C4′methyl hydrogens couple with the aromatic fluorines through space. The methyl hydrogens of C4′ in structure **5b′** are similarly close to fluorine 5 (2.56 Å), but no coupling is observed.

Looking at the CH_3 hydrogens of C1″ in isomer **5b′**, the distances between these hydrogens and fluorines 12 and 13 are *not* within the sum of their Van der Waals radii. Therefore, no through-space coupling would be expected. The experimentally observed doublet of quartets for the analogous CH_2 groups of **5b** instead undoubtedly derives from their diastereotopic nature.

The main reason for the methyl 3-hydroxy-2-but-2-enoate substituent being out of the plane of the aromatic ring is its repulsive interaction with the *syn* fluorine of the closest bridge CF_2 group. Interconversion of isomers **5a′** and **5b′** requires rotation of the C4–C2′ bond through a transition structure where the substituent would be coplanar with the aromatic ring. There are two different possible approaches to such planarity, as shown in, Fig. 6. The first would have the ester moiety interacting with the bridge CF_2 group (**5c′**), whereas the second would have the ketonic methyl group interacting (**5d′**).
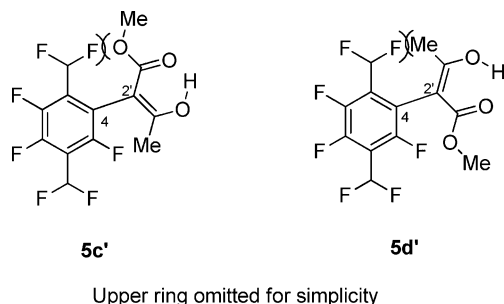
Fig. 6 Possible approaches to planarity through rotation of the C4–C2′ bond.

The lower barrier involved the approach of the ester function (**5c′**), with a calculated rotational energy barrier of 25.2 kcal mol⁻¹ at B3LYP level. This value is in good agreement with that obtained experimentally (23.5 kcal mol⁻¹). The calculated rotational barrier for the alternative approach of the methyl group (**5d′**) was 40.1 kcal mol⁻¹. The transition state for proceeding *via* **5c′** involves having the ester moiety out of the plane of the C2′–C3′ double bond in order to minimize its "contact" with the bridge CF_2 group. Because of the repulsive interaction of the methyl group with the bridge CF_2 group, the alternative rotation *via* **5d′** leads to some elongation and angular distortion of the C4–C2′ bond. This increases the energy for this transition state drastically.

The relative energies for *Away* and *Towards* conformations of cyclized product model system **6′** (methyl ester instead of ethyl ester) have been calculated, with the results given in Fig. 7 below. The furan is perfectly planar with the ring, as expected, with the
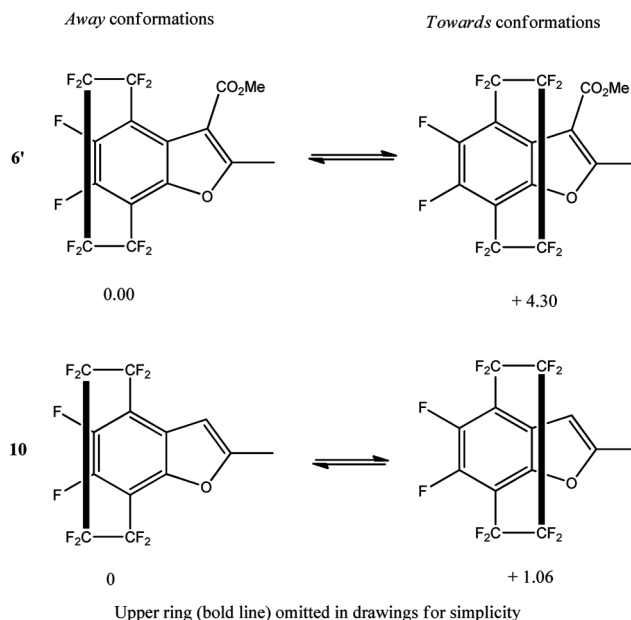
Fig. 7 Calculations of energy differences (kcal mol⁻¹) between *Away* and *Towards* conformations of model systems **6′** and **10**.

Away conformation being more stable by 4.30 kcal mol⁻¹, which is consistent with the NMR results. An issue is whether the bulk of the carbomethoxy group is the reason for the *Away* preference, but it can be seen that the analogous structure without the carbomethoxy group (**10**) also exhibits a preference for the *Away* conformation, albeit with a smaller thermodynamic difference. One must therefore conclude that the lone pair of the furan oxygen does not stabilize the *Towards* conformation by electron donation as much as does the oxygen in a OMe group (previously characterized as *Towards*).[13]

Finally, in order to provide additional insight into the presumed intramolecular S_NAr cyclization process that produces **6** from the enolate of **5**, calculations of this two step process were carried out using a smaller, non-PCP model system, **11** → **13** (Fig. 8). The energy barriers of the transition states for this cyclization process (Fig. 9) were calculated at B3LYP/6-31+G(d,p) level in the presence of THF as a solvent using the Polarizable Continuum Model (PCM).[14]

The transition states were characterized by only one imaginary frequency, and the intrinsic reaction coordinate (IRC). Nucleophilic attack of the enolate (**11**) on the aromatic ring (TS1) has an activation barrier of $\Delta G^{\ddagger} = 29.0$ kcal mol⁻¹. This produces a relatively stable intermediate (**12**) in which the negative charge is delocalized within the electron-deficient ring. The final step is the elimination of the fluoride ion (TS2), which leads to rearomatization and has a calculated activation barrier of $\Delta G^{\ddagger} = 7.3$ kcal mol⁻¹. The product (**13**) of this model reaction is 1.9 kcal mol⁻¹ more stable than starting material **11**.
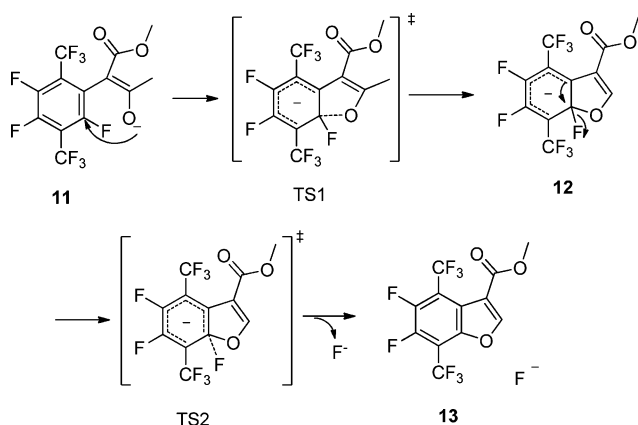
Fig. 8 Proposed mechanism of the cyclization of model system **11** to **13**.
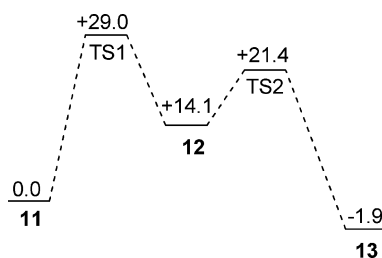

Fig. 9 Energy profile for the cyclization reaction.

Nucleophilic aromatic substitution reactions of highly electron deficient systems such as those of **F8**, hexafluorobenzene, or pentafluoropyridine are generally observed to be low barrier processes, proceeding at room temperature. However, as calculated for the model system, the intramolecular cyclization of **11**→**12**→**13** leads to repulsive interaction of its ester group with the ring CF$_3$ substituent, both at the intermediate stage (**12**) and in the product (**13**). These non-bonded interactions not surprisingly give rise to an increase in the activation energy for the initial cyclization step, with the actual reaction of **5** enolate requiring temperatures above room temperature to occur.

Because the model compound's product (**13**) still has repulsive interactions between a ring CF$_3$ group and the proximate ester moiety, the ester function twists slightly out of plane with consequent loss of conjugation of the ester with the furan ring.

It is expected that the **F8**-furan formation from experimental enolate of **5** would exhibit similar transition states as those shown in Fig. 8 and 9.

Conclusion

In conclusion, the product of S$_N$Ar addition of the enolate of ethyl acetoacetate to perfluoro[2.2]paracyclophane exists entirely as its enol tautomer **5**. This enol exhibits two NMR signals for its enolic proton, and these signals were shown to derive from the presence of two, equal energy conformations that were observable as distinct atropisomers at room temperature, but which when heated, interconverted with an energy barrier of 23.5 kcal mol^{-1}. These atropisomers were characterized by NMR, with computational work corroborating and providing additional insight into all structural, thermodynamic and kinetic results. This enol product **5** was cyclized, under basic conditions, to form a

benzofuran product **6**. The structure of **6** was confirmed by NMR, with further structural and mechanistic insights being provided by calculations.

Experimental section

NMR spectra were obtained in CDCl$_3$ using TMS as the internal standard for ^{1}H (300 MHz) and ^{13}C NMR (75 MHz) and CFCl$_3$ for ^{19}F NMR (282 MHz).

4-(Ethyl 3-hydroxy-2-but-2-enoate)perfluoro[2.2]paracyclophane (5)

To a solution of ethyl acetoacetate (0.45 ml, 3.60 mmol, 4 equiv.) in anhydrous THF (30 mL), 160 mg of NaH (3.96 mmol 4.4 equiv.) 60% in oil suspension were added at room temperature. The solution was stirred at room temperature for 10 min. Then 446 mg of **F8** (0.96 mmol, 1 equiv.) were added and stirred for an additional 24 h at room temperature under nitrogen atmosphere. The reaction was then concentrated to dryness and the residue was purified by column chromatography (hexanes-dichloromethane 3 : 1) to obtain the product as a white solid, 309 mg (56.8%). This analytically pure product was found from its NMR spectra to consist of an approximately 1.5 : 1 mixture of atropisomers, **5a** and **5b**. Details of the proton and fluorine NMR spectra of **5a** and **5b** are provided in Table 1 and in the Supplementary Information.† Anal. Calcd for C$_{22}$H$_9$O$_3$F$_{15}$ C, 43.56; H, 1.50. Found: C, 43.47; H, 1.81.

F8-Furan (6)

To a solution of **5** (100 mg, 0.16 mmol, 1 equiv.) in anhydrous THF (15 mL), 7.8 mg of NaH (0.19 mmol, 1.2 equiv., 60% in oil suspension) were added at room temperature. The solution was stirred at 50 °C for 16 h under nitrogen atmosphere after which the reaction was concentrated to dryness. The residue was purified by column chromatography (hexanes-dichloromethane 2 : 1) to obtain product **6** as a white solid, 51 mg (52.7%). Details of the proton and fluorine NMR spectra of **6** are provided in Table 1 and in the Supplementary Information.† Anal. Calcd for C$_{22}$H$_8$O$_3$F$_{14}$ C, 45.05; H, 1.38. Found: C, 44.75; H, 1.52.

Computational details

Quantum chemical calculations were performed in the gas phase at both HF and B3LYP/6-31+G(d,p) levels of theory. The energy barriers of the transition states towards cyclization were calculated at B3LYP/6-31+G(d,p) level in the presence of THF as a solvent using the Polarizable Continuum Model (PCM). The transition states were characterized by only one imaginary frequency and the intrinsic reaction coordinate (IRC), connecting both the starting material and the product. All calculations were performed using the Gaussian 03 Rev. E01 package.[14]

NMR

All of the NMR spectra, except for the ^{19}F-^{1}H HOESY, were recorded on a three-channel Varian Inova spectrometer, equipped with a 5 mm indirect detection probe, ^{1}H-^{19}F/^{13}C/X, operating at 500 MHz for ^{1}H, and 470 MHz for ^{19}F. The solvent was benzene-d$_6$, and the temperature 25 °C. ^{1}H and ^{13}C chemical shifts were

888 | *Org. Biomol. Chem.*, 2012, **10**, 882–889

This journal is © The Royal Society of Chemistry 2012

referenced to the solvent, 7.14 ppm for ^1H and 128.0 ppm for ^{13}C on the tetramethylsilane scale. ^{19}F chemical shifts were referenced to ϵ = 94.0940478 corresponding to 0 ppm for $CFCl_3$.

^{19}F spectra were recorded with a spectral window from –93 to –140 ppm (22118 Hz) in 16 transients, with an acquisition time of 2 s and a relaxation delay of 0 s, with a 90° pulse width. The FID was zero-filled to 131072 points and weighed with a line broadening function prior to the Fourier transform.

The ^{19}F–^{19}F DQF-COSY spectrum was recorded within a spectral window from –96.3 to 136.2 ppm, which included all of the signals. The number of points for the spectrum was 8192 in both dimensions. The same number of points was acquired in *f2*, in 8 transients per increment, with a relaxation delay of 1 s. The number of increments was 4096. The FIDs were weighted with a line broadening function prior to the Fourier transform.

^{19}F–^1H HOESY spectrum was taken on a Varian Mercury spectrometer, operating at 300 MHz for ^1H and 282 MHz for ^{19}F. The probe was a 5 mm conventional probe, with the high-band coil simultaneously tuned to ^1H and ^{19}F. The 90° pulses were 9.1 and 13.5 μs, correspondingly. Phase-sensitive HOESY spectra were acquired with observation on ^{19}F, in 8192 points, on a spectral window from –64.5 to –208.7 ppm (40984 Hz). The relaxation delay was 1 s, and the number of scans per increment was 64. A number of 512 increments were used in *f1*, on a spectral window from 15 to 0 ppm (4506 Hz). Zero-filling twice to 2048 points was used in *f1*, which afforded a resolution slightly smaller than 2 Hz/point. The mixing time was 0.01 s.

The ^{19}F–^1H heteronuclear nOe difference experiment was run on the Varian Inova spectrometer above, suing the observe channel for ^{19}F and the third channel for ^1H. A power combiner directed the signal of these channels on the high band coil at the probe, tuned to ^{19}F. Te selective irradiation time was 1 s, and the acquisition time 1 s. Spectra were collected in 7500 scans.

The reaction **5a** → **5b** was monitored in benzene-d_6 at 25 °C by ^1H NMR, for 18 h. Spectra were acquired in 64 transients, with a relaxation delay of 10 s and an acquisition time of 10 s, for a total of 51 spectra. Only 40 of them were taken into calculating the rate constant, because in the last ones the mixture was very close to equilibrium and the errors in ln([**5a**]–[**5a**]$_{eq}$) were large. The signals of H1″ were used for integration, after baseline correction.

References

1 L. Zhang, K. Ogawa, I. Ghiviriga and W. R. Dolbier, Jr., *J. Org. Chem.*, 2009, **74**, 6831–6836.
2 V. M. Vlasov, O. V. Zakharova, E. S. Petrov, A. I. Shatenshtein and G. G. Yakobson, *J. Org. Chem. USSR*, 1979, **15**, 123–130.
3 K. Wu, W. R. Dolbier Jr., M. A. Battiste and Y.-A. Zhai, *Mendeleev Commun.*, 2006, 146–147.
4 M. W. Cartwright, E. L. Parks, G. Pattison, R. Slater, G. Sandford, I. Wilson, D. S. Yufit, J. A. A. Howard, J. A. Christopher and D. D. Miller, *Tetrahedron*, 2010, **66**, 3222–3227.
5 M. T. Rogers and J. L. Burdett, *Can. J. Chem.*, 1965, **43**, 1516–1526.
6 J. L. Burdett and M. T. Rogers, *J. Am. Chem. Soc.*, 1964, **86**, 2105–2109.
7 V. P. Kislyi, M. A. Kurykin, V. A. Grinberg, N. D. Kagramanov and V. V. Semenov, *Russ. Chem. Bull.*, 1996, **45**, 2800–2803.
8 J. Kagan, D. A. Agdeppa, D. A. Mayers, S. P. Singh, M. J. Walters and R. D. Wintermute, *J. Org. Chem.*, 1976, **41**, 2355–2361.
9 S. Forsen and R. A. Hoffman, *Acta Chem. Scand.*, 1963, **17**, 1787–1788.
10 S. Forsen and R. A. Hoffman, *J. Chem. Phys.*, 1963, **39**, 2892–2901.
11 Y. Inukai, T. Sonoda and H. Kobayashi, *Bull. Chem. Soc. Jpn.*, 1979, **52**, 2657–2660.
12 G. M. Brooke, W. K. R. Musgrave and T. R. Thomas, *J. Chem. Soc. (C)*, 1971, 3596–3599.
13 I. Ghiviriga, L. Zhang, H. Martinez, R. H. Contreras, C. F. Tormena, L. Nodin and W. R. Dolbier, Jr., *Magn. Reson. Chem.*, 2011, **39**, 93–105.
14 M. J. Frisch, G. W. Trucks, H. B. Schlegel, G. E. Scuseria, M. A. Robb, J. R. Cheeseman, J. Montgomery, J. A. T. Vreven, K. N. Kudin, J. C. Burant, J. M. Millam, S. S. Iyengar, J. Tomasi, V. Barone, M. Bennucci, M. Cossi, G. Scalmani, N. Rega, G. A. Petersson, H. Nakatsuji, M. Hada, M. Ehara, K. Toyota, R. Fukuda, J. Hasegawa, M. Ishida, T. Nakajima, Y. Honda, O. Kitao, H. Nakai, M. Klene, X. Li, J. E. Knox, H. P. Hratchian, J. B. Cross, V. Bakken, C. Adamo, J. Jaramillo, R. Gomperts, R. E. Stratmann, O. Yazyev, A. J. Austin, R. Cammi, C. Pomelli, J. Ochterski, P. Y. Ayala, K. Morokuma, G. A. Voth, P. Salvador, J. J. Dannenberg, V. G. Zakrzewski, S. Dapprich, A. D. Daniels, M. C. Strain, O. Farkas, D. K. Malick, A. D. Rabuck, K. Raghavachari, J. B. Foresman, J. V. Ortiz, Q. Cui, A. G. Baboul, S. Clifford, J. Cioslowski, B. B. Stefanov, G. Liu, A. Liashenko, P. Piskorz, I. Komaromi, R. L. Martin, D. J. Fox, T. Keith, M. A. Al-Laham, C. Y. Peng, A. Nanayakkara, M. Challacombe, P. M. W. Gill, B. Johnson, W. Chen, M. W. Wong, C. Gonzalez and J. A. Pople, *Revision E.01*, Gaussian Inc, Wallingford CT, 2004.